



LAWRENCE
LIVERMORE
NATIONAL
LABORATORY

In-Situ TEM Study of Interface Sliding and Migration in an Ultrafine Lamellar Structure

Luke Hsiung

December 7, 2005

Journal of Materials Research

Disclaimer

This document was prepared as an account of work sponsored by an agency of the United States Government. Neither the United States Government nor the University of California nor any of their employees, makes any warranty, express or implied, or assumes any legal liability or responsibility for the accuracy, completeness, or usefulness of any information, apparatus, product, or process disclosed, or represents that its use would not infringe privately owned rights. Reference herein to any specific commercial product, process, or service by trade name, trademark, manufacturer, or otherwise, does not necessarily constitute or imply its endorsement, recommendation, or favoring by the United States Government or the University of California. The views and opinions of authors expressed herein do not necessarily state or reflect those of the United States Government or the University of California, and shall not be used for advertising or product endorsement purposes.

IN-SITU TEM STUDY OF INTERFACE SLIDING AND MIGRATION IN AN ULTRAFINE LAMELLAR STRUCTURE

L. M. Hsiung
Lawrence Livermore National Laboratory
Chemistry and Materials Science Directorate
L-352, P.O. Box 808
Livermore, CA 94551-9900, USA.

Abstract

The instability of interfaces in an ultrafine TiAl-(γ)/Ti₃Al-(α_2) lamellar structure by straining at room temperature has been investigated using in-situ straining techniques performed in a transmission electron microscope. The purpose of this study is to obtain experimental evidence to support the creep mechanisms based upon the interface sliding in association with a cooperative movement of interfacial dislocations previously proposed to interpret the nearly linear creep behavior observed from ultrafine lamellar TiAl alloys. The results have revealed that both the sliding and migration of lamellar interfaces can take place simultaneously as a result of the cooperative movement of interfacial dislocations.

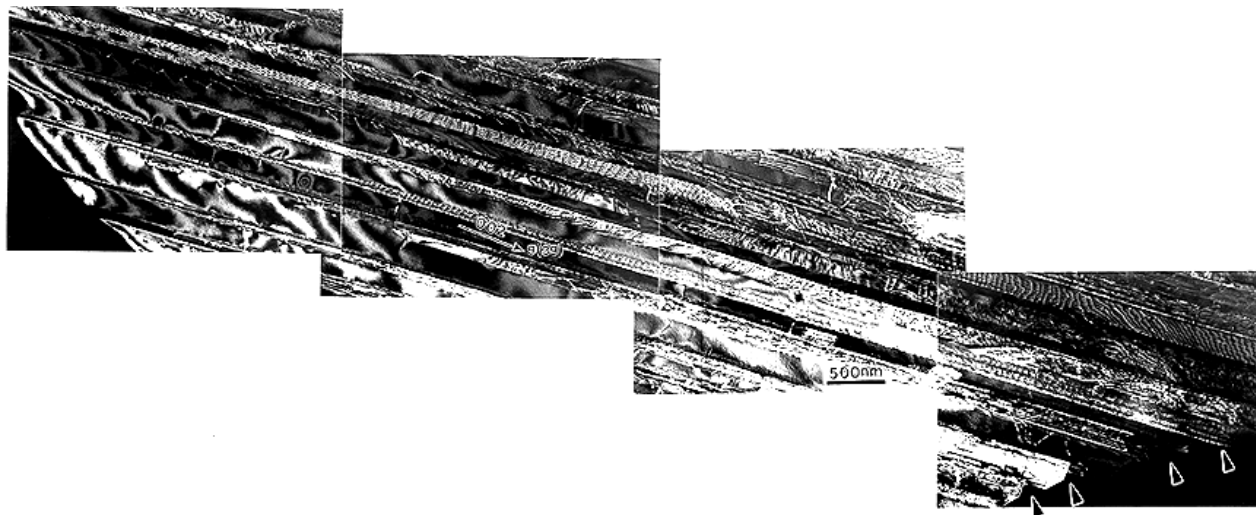
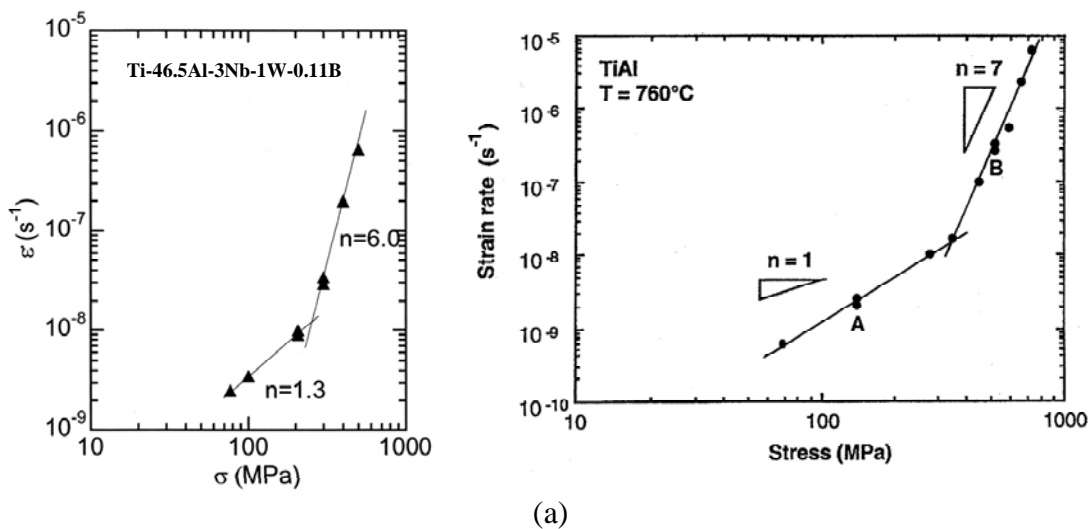
Introduction and background

It has been reported that the mobility of interfacial dislocations can play a crucial role in the creep deformation behavior of ultrafine TiAl-(γ)/Ti₃Al-(α_2) lamellar alloys [1-5]. Since the operation of lattice dislocations within refined γ and α_2 lamellae is largely constrained, interfacial dislocations become the major strain carriers for plasticity. As shown in Figs. 1 (a) and (b), a nearly linear creep behavior [i.e. $\dot{\epsilon}$ (steady-state creep rate) = $k\sigma^n$, where σ is applied creep stress and $n \approx 1$] was observed in low-stress (*LS*) regime, and a power-law breakdown ($n > 5$) was observed in high-stress (*HS*) regime of two lamellar TiAl alloys with different compositions [4,5]. Results of TEM investigation as shown in Figs. 1 (c) and 1 (d) have indirectly revealed the occurrence of interface sliding in low-stress (*LS*) creep regime and deformation twinning in high-stress (*HS*) creep regime. These results have led us to propose that interface sliding associated with a viscous glide of pre-existing interfacial dislocations is the predominant creep mechanism in *LS* regime and interface-activated deformation twinning in γ lamellae is the predominant creep mechanism in *HS* regime [1, 2]. Stress concentration resulting from the movement and pileup of interfacial dislocations has been suggested to be the cause for the interface-activated deformation twinning. Accordingly, the creep resistance of ultrafine lamellar TiAl alloys is considered to depend greatly on the cooperative movement of interfacial dislocations, which in turn may be controlled and hindered by the interfacial segregation of solute atoms (such as W) or interfacial precipitation [3-5]. Furthermore, through the in-situ TEM observation, we have also found that the lamellar interfaces can migrate directly through the cooperative motion of interfacial dislocations. That is, the γ/γ and γ/α_2 interfaces can migrate through interface sliding and lead to the coalescence or shrinkage of constituent lamellae (i.e. microstructural instability), which results in a weakening effect when ultrafine lamellar TiAl is employed for engineering applications. Although it is anticipated that the interface sliding and migration are prevalent at elevated temperatures, the present in-situ straining study reveals the instability of lamellar interfaces, in particular the γ/γ interfaces, at ambient temperatures.

Experimental

A TiAl-(γ)/Ti₃Al-(α_2) two-phase lamellar alloy with a nominal composition of Ti-47Al-2Cr-1Nb-1Ta (at.%) was fabricated by a powder metallurgy process, which involves a hot-extrusion of gas-atomized titanium aluminide powder (particle size: - 200 mesh) canned in molybdenum billets. The

hot-extrusion was conducted at 1400 °C. After extrusion, the rod-shape alloy was stress-relieved at 900°C for 2h in a vacuum of $\sim 10^{-4}$ Pa. TEM foils were prepared by twin-jet electropolishing in a solution of 60% methanol, 35% butyl alcohol and 5% perchloric acid at 15V and -30°C. Interfacial substructures were examined using JEOL-200CX transmission electron microscope. Dislocation structure and the core structure of interfacial dislocations were also examined using high-resolution (HRTEM) imaging techniques. To investigate strain-induced interface migration, an in-situ straining experiment was performed at room temperature in a JEOL-200CX transmission electron microscope using a single-tilt straining holder. A gear-drive translation mechanism was activated through the foot pedals with the deformation rate controlled by the speed of y-axis tilt. Plastic deformation took place and was recorded right after a short period of time in which elastic deformation was first distinguished from the motion of bend extinction contours. A hi-8 videocassette recorder attached to a TV rate camera in the microscope was used to record the straining events (e.g., dislocation motion/interaction, interface migration). After completing the experiment, video images of special interest were printed out for analysis.



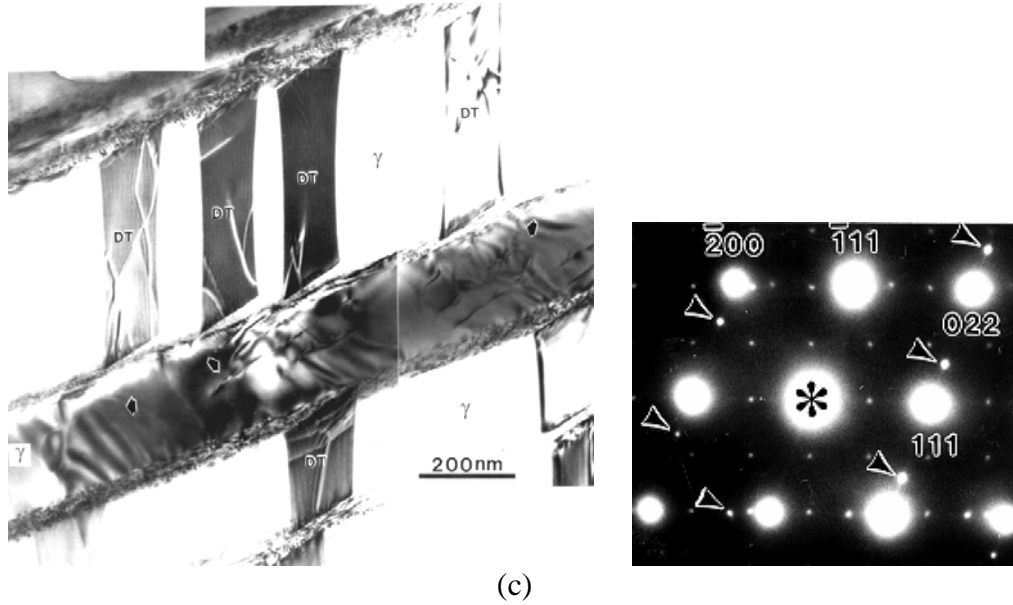


Fig. 1. (a) Steady-state creep rate plotted as a function of applied stress at 760 °C for Ti-46Al-3Nb-1W (left) and Ti-47Al-2Cr-2Nb (right) lamellar alloys showing the existence of two distinct low-stress and high-stress creep regimes; (b) a TEM image showing the formation of grain boundary ledges (marked by arrows) resulted from the interface sliding within a specimen creep-deformed at 138 MPa [condition A in (a)]; (c) a bright-field TEM image showing the formation of $(\bar{1}11)$ type deformation twins (*DT*) within a specimen creep-deformed at 518MPa [condition B in (a)].

Results and Discussion

There are in general two types of lamellar interfaces within fully lamellar TiAl [6-8], i.e. (1) the γ/α_2 interphase interface which has the orientation relationship: $(0001)_{\alpha_2} \parallel (111)_{\gamma}$ and $\langle 11\bar{2}0 \rangle_{\alpha_2} \parallel \langle 1\bar{1}0 \rangle_{\gamma}$, and (2) the γ/γ interfaces which include true twin, pseudo twin, and order-fault interfaces. Types (2) interface is also referred as twin-related interfaces hereafter. A typical TEM observation of lamellar interfaces viewed from the $[011]_{\gamma}$ edge-on orientation is shown in Fig. 2. Notice that interfacial dislocations can be found in both γ/γ and γ/α_2 interfaces. Figure 2(b) was imaged with a tilting angle of $\sim 15^\circ$ from Fig. 2(a). Several dislocation tips (appeared as white dots) in Fig. 1(a), and the corresponding dislocation lines appeared in Fig. 2(b) are marked by arrows. In general, the dislocation density in γ/α_2 interphase interfaces is higher than that in γ/γ twin-related interfaces as a result of a greater lattice and thermal misfit between γ and α_2 lamellae. The core of each interfacial dislocation in γ/α_2 interface contains an atomic ledge (step) with the ledge height two layer thickness of the $(111)_{\gamma}$ plane ($d_{111} = 0.232$ nm) is shown in Fig. 3(a), which is consistent with the observations reported elsewhere in literature [9, 10]. Similar properties are also true for γ/γ_T interfaces, and an atomic ledge is associated with the core of each interfacial dislocation ($\mathbf{b} = 1/6[\bar{1}\bar{1}2]$) in γ/γ_T interface with the ledge height one layer spacing of the $(111)_{\gamma}$ plane [Fig. 3(a)]. Accordingly, if an interfacial dislocation moves along the interface, the ledge moves along with the dislocation and thus, the interface is displaced (advanced) perpendicular to its plane, i.e. the interface will migrate by the distance of a ledge-height. Therefore, the cooperative motion of interfacial dislocations will always cause a combination of interface sliding and interface migration as illustrated schematically in Fig. 4(a) and Fig. 4(b) for γ/α_2 and γ/γ_T interfaces, respectively. Since the Burgers vector ($\mathbf{b} = 1/6[\bar{1}\bar{1}2]$) of interfacial dislocations is parallel to the $(111)_{\gamma}$ plane, the dislocations need only to glide to cause the interface to slide. The interfacial dislocations in γ/γ_T true-twin interface compensate a small angle departure of the γ/γ_T interface plane from the exact (111) twin plane, which is schematically illustrated in Fig. 4 (b). The inclination angle (θ) of the interface plane to the exact twin plane is therefore given

by eqn. (1): $\tan \theta = \frac{h}{s}$, where, h is the step height, and s is the average spacing of interfacial dislocations.

Accordingly, it is anticipated that the cooperative movement of interfacial (Shockley partial) dislocations can result in the migration of lamellar interfaces, and thereby lead to the coalescence/shrinkage of the constituent lamellae. The migration rate (v_i) of an interface can be expressed as eqn. (2): $v_i = \rho v_d h$, where ρ is the dislocation density, v_d the dislocation velocity, and h the step height.

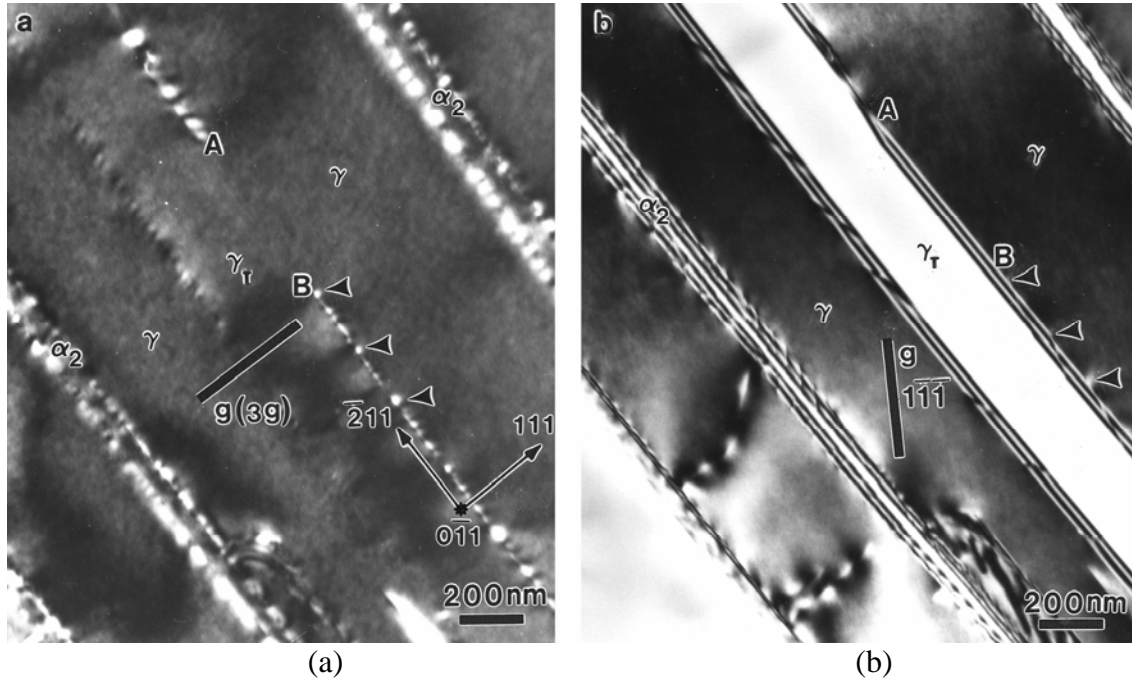


Fig. 2 (a) A WBD TEM image showing a typical edge-on lamellar structure consisting of γ , γ_T and α_2 lamellae within an as-fabricated alloy sample, Z (zone axis) = $[0\bar{1}1]_\gamma$; (b) A bright-field TEM image showing the existence of interfacial dislocations in both γ/α_2 and γ/γ_T interfaces, $Z = [1\bar{2}1]_\gamma$.

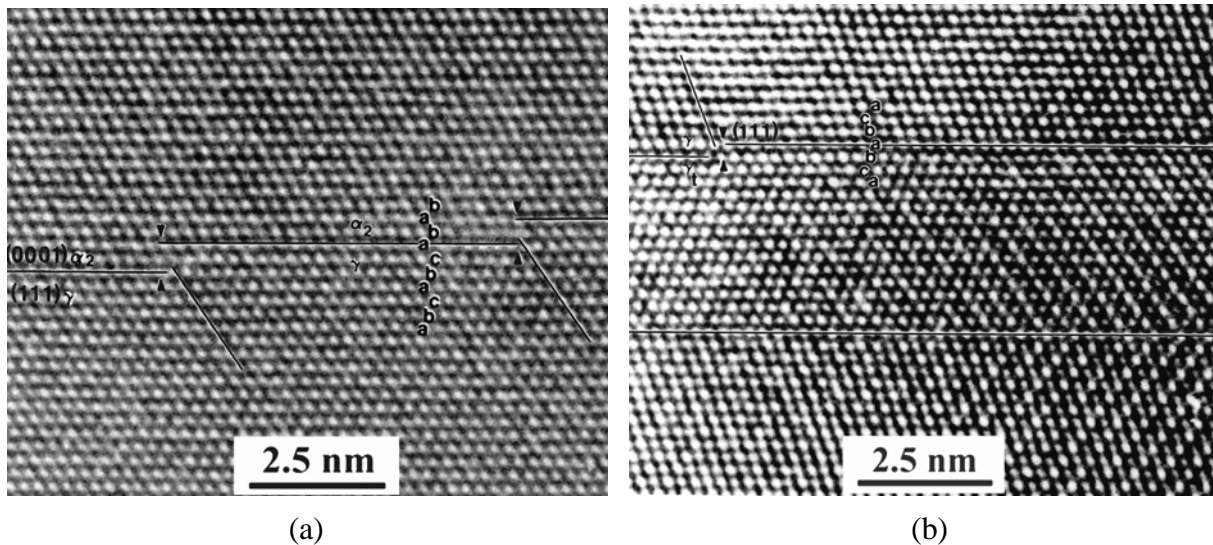


Fig. 3. HRTEM images showing the core structure of interfacial dislocations in (a) γ/γ_T and (b) γ/α_2 interfaces. The letters **abab** and **abcabc** stand for the stacking sequence of α_2 and γ lamellae, respectively. Notice that an atomic ledge is associated with the core of interfacial dislocation.

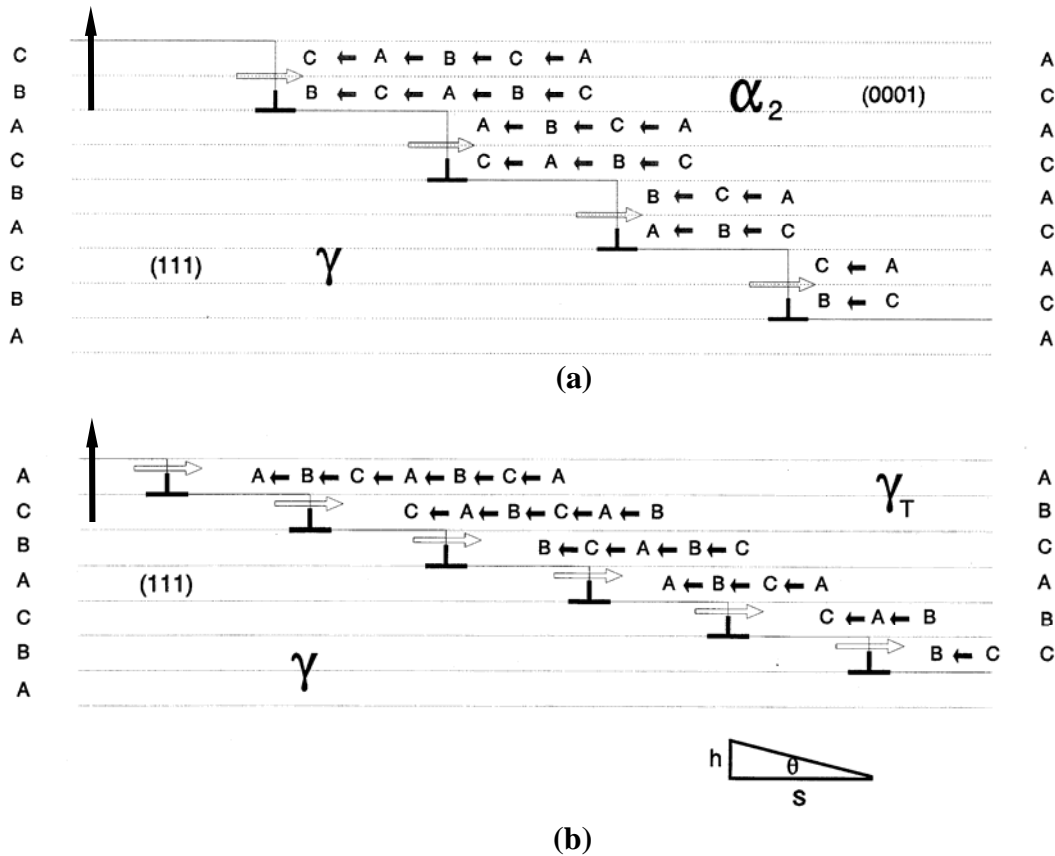


Fig. 4. Schematic illustrations of (a) an array of interfacial (Shockley partial) dislocations forming a glissile α_2/γ interface and (b) an array of interfacial (Shockley partial) dislocations in a glissile γ/γ_T interface. Both interfaces can be migrated by the cooperative motion of the interfacial dislocations. The letters **ACAC** and **ABC** stand for the stacking sequence of α_2 -lamella and γ -lamella, respectively. The direction of interface migration is indicated by an arrow (\uparrow).

Interface sliding

A direct observation of interface sliding and migration has been obtained successfully from an in-situ straining experiment. Throughout the in-situ straining experiment, which was conducted at room temperature, the motion of interfacial dislocations was mainly observed in γ/γ twin-related interfaces. This indicates that the mobility of interfacial dislocations in γ/α_2 interfaces is much lower than that of interfacial dislocations in γ/γ twin-related interfaces at room temperature. Typical video images recorded from the in-situ straining experiment for the motion of interfacial dislocations in a pair of edge-on twin interfaces are demonstrated in Figs. 5 (a) and (b), in which the specified interfacial dislocations are marked by arrows. It is seen that dislocations in the left interface moved cooperatively about 52 nm downward after 35 seconds, while the dislocations in the right interface moved about 38 nm upward, which is slower than those in the left interface. The average dislocation velocity (v_d) is estimated to be 1.5 nm/sec for those in the left interface and 1.1 nm/sec for those in the right interface. With a known dislocation density at the interface ($\rho \sim 0.033 \text{ nm}^{-1}$), the interface migration rate (v_i) can be evaluated [according to eqn. (2)] to be 0.008 nm/sec - 0.012 nm/sec, which is so slow that the interface migration is not detectable within a short period of time.

Figure 6 shows the result of another in-situ TEM experiment, which reveals the movement of interfacial dislocations during electron-beam heating of a thin foil (prepared from a sample creep deformed at 760°C and 138MPa) contained residual stress. The original idea of the experiment was assuming that the relaxation of residual stress could result in the movement of interfacial dislocations,

and the local heating could be obtained when electron-beam was focused to a small spot size of several micron meters. Since the purpose of this study is to demonstrate the direct observation of the movement of interfacial dislocation, how high the temperature can be increased by the beam heating is not a concern. The cooperative motion of a dislocation array of eight interfacial dislocations on an inclined interface can be readily seen in Fig. 6. The movement of each dislocation was in a viscous drifting or pinning/unpinning fashion, and each of the dislocations had a different drifting velocity. Here, the #1 leading dislocation of the array moved about 375 nm, and the #8 trailing dislocation moved about 425 nm after beam heating for 30 seconds. This reveals that each interfacial dislocation can have different mobility as a result of a solute-dragging effect.

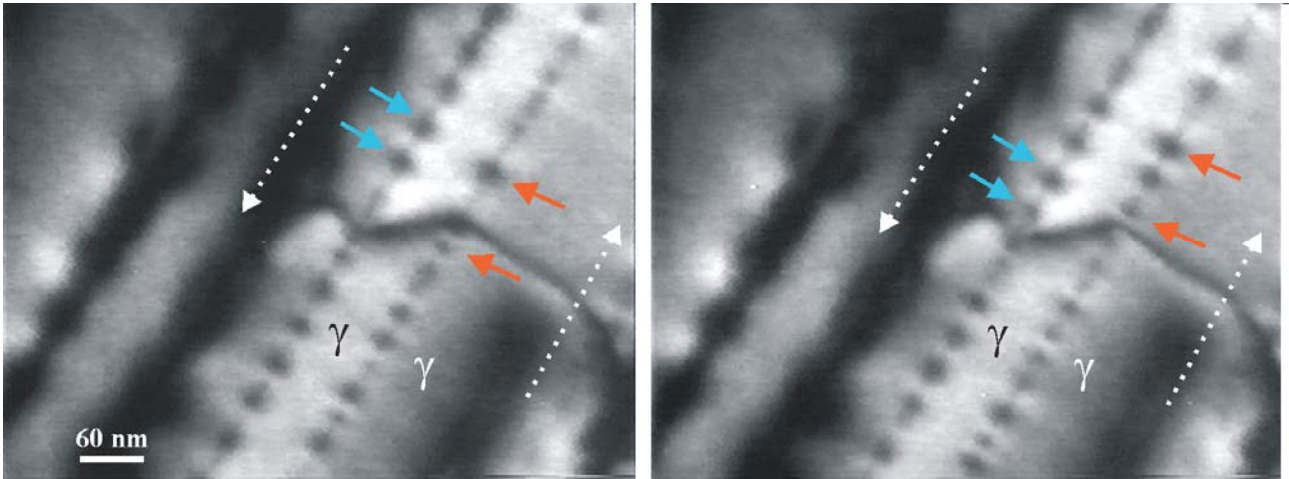


Fig. 5. Two consecutive in-situ video images showing the cooperative motion of interfacial dislocation tips (appeared as black dots) in a pair of γ/γ interfaces; the moving directions are labeled by long arrows.

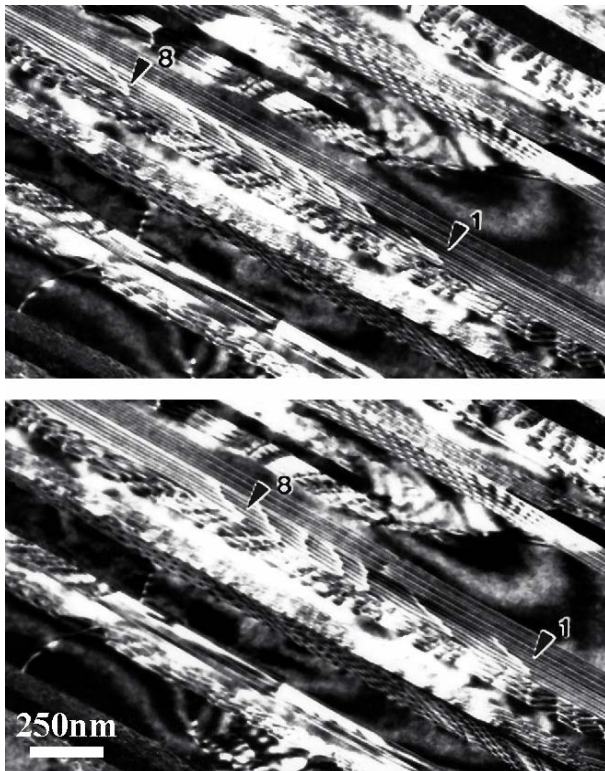


Fig. 6. Two consecutive in-situ TEM images show the cooperative movement of interfacial dislocation (driven by beam heating) in a lamellar interface (time lapse for beam heating: 30 seconds).

Stress-induced interface migration

An in-situ observation of interface migration is demonstrated in Figs. 7 (a) – 7 (d), in which the images were recorded in a region close to a crack tip. It is interesting to note that the velocity of dislocation motion in a γ/γ twin-related interface is found to be much faster than that observed in Fig. 5 as a result of the existence of a stress concentration adjacent to the crack tip. In fact, the dislocation velocity is so fast that it becomes difficult to track the motion of individual dislocation. However, the velocity of dislocation motion can be evaluated indirectly according to eqn. (2) by measuring the rate of interface migration. Here, the interface initially migrated in an average rate of $v_i \sim 0.4$ nm/sec [Figs. 7 (a) and 7 (b)], which is corresponding to a dislocation velocity of $v_d \sim 50$ nm/sec. After 40 seconds the migration rate suddenly increases to $v_i \sim 9$ nm/sec [Figs. 7 (b) and 6(c)] by moving the interfacial dislocations in a bursting fashion, which is corresponding to a dislocation velocity of $v_d \sim 1,125$ nm/sec. After 43 seconds the average migration rate decreases to $v_i \sim 0.6$ nm/sec [Figs. 7 (c) and 7 (d)], i.e. $v_d \sim 75$ nm/sec. The interface subsequently migrates close to another lamellar interface, and the migration rate further decreases as a result of the interaction of stress field between two interfaces. The result of coarsening or de-twinning is readily evidenced here because of the stress-induced migration of the γ/γ twin-related interface.

Summary

Stress-induced interface sliding and migration in lamellar TiAl have been directly observed using in-situ straining techniques performed in a transmission electron microscope. The results clearly show that the interfacial dislocations in a certain lamellar interfaces are mobile even at room temperature. Since step (ledge) is associated with the core of each interfacial dislocation, the lamellar interfaces can thus migrate through the cooperative motion of interfacial dislocations, which results in the microstructural instability (coarsening/shrinkage) of constituent lamellae. Both the dislocation velocity and migration rate are very sensitive to the magnitude of resolved shear stress acting on the interfaces. The results of current study reveal that to appropriately control the mobility of interfacial dislocation is of paramount importance for the enhancement of both microstructural stability and creep resistance of ultrafine lamellar TiAl especially at elevated temperatures.

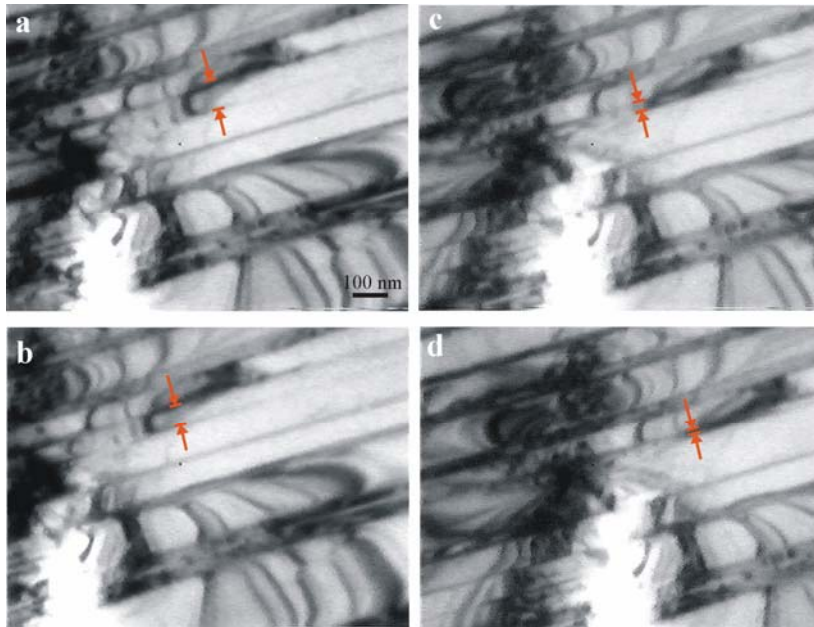


Fig. 7. Consecutive in-situ video images showing the migration of a twin-related interface near a crack tip; (a) $t = 0$, (b) $t = 40$ sec, (c) $t = 43$ sec, (d) $t = 70$ sec.

Acknowledgements – This work was performed under the auspices of the U.S. Department of Energy by University of California, Lawrence Livermore National Laboratory under contract No. W-7405-Eng-48. The author would like to thank Dr. Adam Schwartz and Mr. M. A. Wall for their technical advice in carrying out the *in situ* straining experiment. The authors are also in debt to Prof. T. G. Nieh of the University of Tennessee and Dr. C. T. Liu of Oak Ridge National Laboratory for their technical guidance and providing the alloys used for this investigation.

References

1. L. M. Hsiung and T. G. Nieh, *Intermetallics* **7**, 821 (1999).
2. L. M. Hsiung, T. G. Nieh, B.W. Choi, and J. Wadsworth, *Mater. Sci. Eng.*, A329-331, (2002), 637.
3. L. M. Hsiung, Mat. Res. Soc. Symp. Proc., MRS, 740, p. 287 (2003).
4. L. M. Hsiung and T. G. Nieh, *Mater. Sci. and Eng.* **A364**, p. 1 (2004).
5. A. M. Hodge, L. M. Hsiung and T. G. Nieh, *Scripta Mater.*, **51** (2004), 411.
6. M. Yamaguchi and Y. Umakoshi, *Progress in Materials Science*, **34**, 1 (1990).
7. M. Yamaguchi and H. Inui, in *Structural Intermetallics*, ed. R. Darolia *et al.*, TMS, Warrendale, PA, 127(1993).
8. Y. Yamamoto, M. Takeyama, T. Matsuo, *Mater. Sci. Eng.*, **A329-331** (2002), 631.
9. L. Zhao and K. Tangri, *Phil. Mag. A*, **65** (1992), 1065.
10. G. J. Mahon and J. M. Howe, *Metall. Trans. A*, **21A** (1990), 1655.